New CLEO Results on Tau Physics

Brian K. Heltsley, Cornell University
On behalf of the CLEO Collaboration

ABSTRACT

New, preliminary tau physics results are reported from tau-pair data acquired with the CLEO II detector operating at the Cornell Electron Storage Ring. The tau mass is measured as $m_\tau = 1777.6 \pm 0.9 \pm 1.5$ MeV/c^2 by exploiting the kinematics of events in which both taus decay hadronically. The electronic branching fraction is determined to be $\mathcal{B}_e$=0.1742±0.0015±0.0023 by counting di-electron tau-pair decays and normalizing to luminosity. Using a similar double-tag method, we measure the branching fraction for a single charged hadron $h^\pm$ ($\pi^\pm$ or $K^\pm$) accompanied by exactly one π^0 as $\mathcal{B}(h^\pm\pi^0\nu)$= 0.2483±0.0015±0.0053. Branching fractions to $h^\pm$ accompanied by two, three, or four π^0's, normalized to $\mathcal{B}(h^\pm\pi^0\nu)$, are also presented as 0.348 ±0.006 ±0.016, 0.042 ±0.003 ±0.004, and 0.006 ±0.002 ±0.002, respectively.

I. Introduction

Since discovery of the tau, most measurements have shown that it behaves as a sequential heavy lepton as predicted by the Standard Model of electroweak interactions. The latest generation of improved detectors has been called upon to resolve two nagging discrepancies from theoretical expectations. The "consistency problem" (or "lifetime puzzle"), in which the measured tau mass, lifetime, and electronic branching fraction fail to conform to leptonic universality, could be a harbinger of new physics[4, 5] or a hint to experimentalists to more closely examine their systematics. The "one-prong problem,"[1, 2, 3] wherein measured exclusive modes fail to saturate the inclusive one-charged-particle decay width, indicates either subtle experimental difficulties or the presence of unexpected decay modes. This work presents for the first time new, preliminary tau physics results from CLEO II that bear directly on both "problems." Updated results should be published during the next few months.[6]

Earlier this year ARGUS reported[7] m_τ=(1776.3±2.4±1.4) MeV/c^2, significantly below the previous world average[3] value of $(1784.1^{+2.7}_{-3.6})$ MeV/c^2. Shortly thereafter the BES experiment presented a precision mass measurement[8] of (1776.9±0.4±0.3) MeV/c^2, corroborating the indications from ARGUS. Section II explains a new technique used on CLEO data to extract a tau mass confirming the lower value. Unfortunately, though the reduction reduced (temporarily) the significance of the consistency problem, it did not go nearly far enough to resolve the issue.

The electronic branching fraction ($\mathcal{B}_e$) of the tau lepton enjoys a special role in the Standard Model of electroweak interactions as applied to tau decay. The theory[9] explicitly relates $\mathcal{B}_e$ to the tau mass m_τ and lifetime τ_τ. Many of the tau branching fractions (for $\tau \to \mu\nu\bar{\nu}$, $\pi\nu$, $K\nu$, $\rho\nu$, $K^*\nu$, and $4\pi\nu$) can be expressed [2, 9, 10, 11] as $\mathcal{B}_e$ times multiplicative factors which include low energy experimental results. To enable more precise tests of these predictions, we present in Section III a new measurement of $\mathcal{B}_e$ with substantially smaller errors than any previous single experiment.

The largest decay mode of the tau is to one charged pion and one π^0. The branching fraction for this mode is not precisely known, with measured values ranging from 22% to 25%.[3] Section IV details an analysis yielding the most precise measurement of this branching ratio to date.

The existing data for branching ratios of tau decays to final states containing multiple π^0's have been also relatively imprecise.[3] Section V presents new measurements of the branching fractions $\mathcal{B}(h^\pm n\pi^0\nu)$ for $n = 2$ and 3, and the first measurement of $\mathcal{B}(h^\pm 4\pi^0\nu)$, where $h^\pm$ represents a charged hadron ($\pi^\pm$ or $K^\pm$). The branching fractions from this analysis are normalized to $\mathcal{B}(h^\pm\pi^0\nu)$ since many potential systematic errors tend to cancel.

For all four analyses in this work, tau-pair production and decay properties (such as reconstruction kinematics, efficiencies for specific decay modes, and "feed-across" from other tau decay modes) are calculated using the KORALB[12] $\tau^+\tau^-$ event generator with a detector simulation based on the GEANT[13] package. Beam-related detector hits are simulated by embedding random trigger events into the Monte Carlo raw data.

CLEO II is a general purpose detector[14] operating at the Cornell Electron Storage Ring (CESR) at e^+e^- center-of-mass energies near the Υ(4S) resonance ($\sqrt{s}$ =E_{cm}=2E_{bm}≃10.6 GeV). The detector components central to these analyses are the tracking system and calorimeter. Wire drift chambers in a 1.5 T axial magnetic field provide charged particle momentum measurements with resolution σ_p/p (%) $\simeq \sqrt{(0.15p)^2 + (0.5)^2}$, p in GeV/c, and ionization loss determination that has 6.2% resolution on beam energy electrons. Inside the superconducting magnet coil an array of 7800 CsI(Tl) crystals is divided into a barrel region and two endcaps. The 6144 barrel crystals, arranged in a projective geometry, surround the tracking chambers at ∼1 m radius, covering $|\cos\theta| < 0.82$, where θ is the polar angle with respect to the positron beam direction. Two identical endcaps, each composed of 828 rectangular crystals, complete the hermetic coverage over 98% of the solid angle by covering the region $0.80 < |\cos\theta| < 0.98$. The barrel calorimeter achieves energy and angular resolutions, respectively, of σ_E/E (%) $= 0.35/E^{0.75} + 1.9 - 0.1E$ and σ_ϕ (mrad)=$2.8/\sqrt{E} + 2.5$, E in GeV. Muons are detected by their penetration through part or all of the ∼1 meter of iron surrounding the calorimeter, which has three equally-spaced gaps in depth, each instrumented with three wire-chamber layers.

II. Measurement of the Tau Mass

The novel method used here to measure the tau mass exploits the kinematics in the e^+e^- center-of-mass of tau-pair production and decay, as well as the power of CLEO II. If a detector can fully reconstruct all decay products except the neutrino in a non-leptonic tau decay, energy-momentum conservation constrains the unknown tau direction to lie on a cone around the detected hadronic system's net momentum vector. This cone's half-angle depends upon the hadronic four-momentum and the tau mass and energy. In the absence of initial state radiation, both of the two taus have the beam energy E_{bm} and

emerge from the collision back-to-back. In a tau-pair event wherein *both* decay hadronically, the original tau directions must lie on one of the two rays formed by the intersection of the cone from one tau decay and the parity-inversion of the cone from the other. Both cone half-angles will shrink if the tau mass is reduced; eventually, the two cones just touch. Since further reduction of the tau mass yields tau directions which cannot be back-to-back, this degenerate solution is the "minimum kinematically allowed tau mass" for the event, M_{min}. A simple quadratic equation can be solved for the value of M_{min} in events where both taus have fully reconstructed hadronic decays.

Monte Carlo studies[12] predict that in a perfect detector the M_{min} distribution exhibits a pileup of events just below the tau mass, followed by a sharply falling edge and a very small high-mass tail. In the non-ideal case, several factors can contribute to a softening of the sharp edge, to the high-mass tail, and potentially to a change in the position and slope of the edge: initial and final state radiation; missing or unreconstructed particles; misidentification of leptonic decays; uncertainty in the knowledge of the neutral energy and charged momentum scales for the detector; background from non-tau-pair events; detector resolution smearing of the kinematic quantities; π/K misidentification and other mismeasurements of the hadronic system; uncertainty in the knowledge of the beam energy and the beam energy spread; and uncertainty in the knowledge of the tau neutrino mass.

Events are selected in which both taus decay hadronically to one charged particle and 0, 1, or 2 π^0's. Compared with other topologies, these 1-vs-1 events with π^0's are relatively free of hadronic background and have large branching ratios. Topologies involving three charged particle decays have not yet been used; they will have somewhat less statistical power, higher background, more dependence on the momentum scale, and less dependence on the calorimeter energy scale.

Events are required to have exactly two reconstructed charged tracks of opposite charge and separated in angle by $\geq 90°$. Both tracks must have more than 100 MeV/c of momentum transverse to the beam. To reject Bhabhas, no more than one track can have momentum exceeding $0.85E_{bm}$ and the total visible energy in the calorimeter must be less than 85% of E_{cm}. Showers in the calorimeter are used to make π^0's if they are unmatched to the charged tracks, lie in the barrel region ($|\cos\theta| < 0.71$), and have energy > 40 MeV. Shower pairs must lie within three standard deviations of the π^0 mass ($\sigma_{\gamma\gamma} \simeq$ (5-9 MeV/c^2). Defining the quantity $S_{\gamma\gamma} \equiv (m_{\gamma\gamma} - m_{\pi^0})/\sigma_{\gamma\gamma}$, this cut corresponds to $|S_{\gamma\gamma}| < 3$. The event is rejected if any unused neutral showers of more than 100 MeV remain. Each reconstructed π^0 is then associated with the charged track nearest to it in space angle. No more than two π^0's may be associated with each charged track, and there must be at least one π^0 in each event.

To reject leptonic decays, a charged track unassociated with π^0's must leave a shower in the calorimeter with energy less than 85% of its momentum (to reject $e^{\pm}$), and not penetrate four interaction lengths of material in the outer muon detection system (to reject $\mu^{\pm}$). In order to reject background from two-photon physics, the visible energy in the event (charged tracks and π^0's) must exceed $0.4E_{cm}$, and the visible momentum transverse to the beam must exceed 500 MeV/c.

If an event appears with more than one valid combination of photons in π^0's, both combinations are used in the analysis; this happens less than 1% of the time. For each valid $\gamma\gamma$ combination, the π^0's are kinematically constrained to the π^0 mass. The four-vectors of the two hadronic systems are formed, from which the value of M_{min} is calculated. Approximately 8% of all events are discarded because the visible energy of a hadronic system is larger than the beam energy, or its invariant mass is larger than M_{min}.

In a dataset with total luminosity 1.43fb^{-1}, corresponding to 1.31M produced tau-pairs, a total of 28892 combinations pass all cuts. The M_{min} distributions are shown in Fig. 1. The predicted pileup just below the tau mass, the sharp drop, and the high-mass tail are all evident. The shape of the M_{min} distribution is the same in both data and Monte Carlo. The Monte Carlo pre-

dicts that events in the high-mass tail have either hard initial state radiation or unreconstructed or misidentified particles.

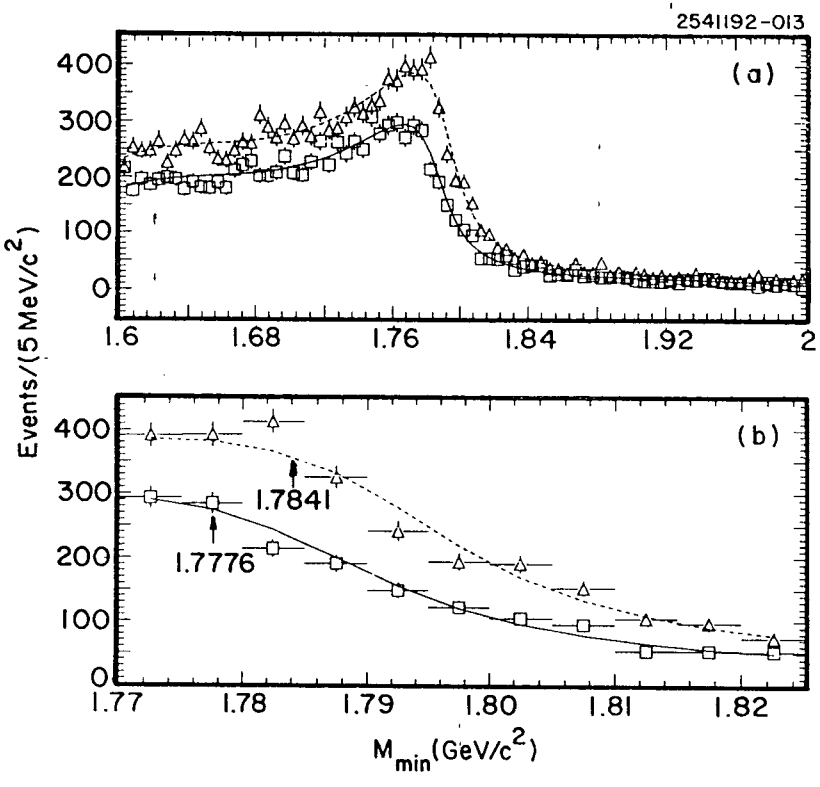

Fig. 1. (*a*) The M_{min} distribution and fit for the data (squares, solid curve) and in the Monte Carlo (triangles, dashed curve). (*b*) An expanded view of M_{min}. The Monte Carlo was generated with a mass of 1.7841 GeV/c^2. The arrows show the location of the fitted tau mass. The vertical scale for the Monte Carlo is arbitrary.

Both the data and Monte Carlo M_{min} distributions are fitted with an empirical shape, composed of an arctangent curve, falling from 1 to 0 in the vicinity of the edge, with its position and slope as fit parameters; a fourth-order polynominal multiplying the arctangent to model the falloff at masses below the edge; and a first-order polynominal to model the high-mass tail. The parameters governing the two polynomials are determined from the M_{min} distribution in the Monte Carlo. Only the overall normalization and position of the arctangent curve are varied to fit the data. The fits are shown as superimposed curves on Fig. 1. Here, a tau mass of 1784.1 MeV/c^2 was used in the Monte Carlo. The fitted position of the edge in Monte Carlo depends linearly on the input tau mass over the entire range of interest.

From Monte Carlo simulations, background from hadronic events ($B\overline{B}$ and continuum) are expected to be negligible. Background from two-photon events is less than 1%. None of these backgrounds produce structure in the M_{min} distribution near the tau mass.

Uncertainties in neutral or charged particle measurements can potentially lead to changes in the position and slope of the edge in the M_{min} distribution, as can slight variations in the beam energy, the event selection criteria, or the fitting procedure. A non-zero tau neutrino mass also alters the resulting tau mass. The contributions to the systematic error are summarized in Table 1, in which the uncertainty in each important variable v are listed along with the observed slopes dm_τ/dv and the resulting error assignment in m_τ.

Table 1: Sources of Error in the Tau Mass Measurement

Variable v	dm_τ/dv	Δv	Δm_τ (MeV/c^2)
Calorimeter energy	4 MeV/%	±0.3%	1.2
Momentum	8 MeV/%	±0.1%	0.8
Beam energy	3 MeV/%	±0.03%	0.1
Vary cuts	–	–	0.5
Tau neutrino mass	–	+35 MeV	0.9

The dependence of the fitted mass on shifts of scale (dm_τ/dv) was determined by varying the appropriate scale, in both data and Monte Carlo, and

refitting the M_{min} distributions. The dependence of the edge position on fractional changes of scale was in good agreement between data and Monte Carlo for all variables. The calorimeter energy scale is established by comparing the position of the mass peak in the decay $\pi^0 \to \gamma\gamma$ in data and Monte Carlo. The momentum scale in data and Monte Carlo is established by measuring the position of mass peaks in hadronic events from the decays $K_S \to \pi^+\pi^-$, $D^0 \to K^-\pi^+$, $D^+ \to K^-\pi^+\pi^+$, $\Lambda \to p^+\pi^-$, and $J/\psi \to \mu^+\mu^-$. A tau neutrino mass different from zero will shift the position of the edge; the shift is quadratic in the neutrino mass.

The final result is $m_\tau = 1777.6 \pm 0.9 \pm 1.5^{+0.9}_{-0.0}$ MeV/c^2, where the errors are from statistics, systematics, and uncertainty on the tau neutrino mass, respectively. This measurement agrees well with the recent measurements from BES[8] and ARGUS.[7]

Mass measurements made at $\tau^+\tau^-$ threshold are independent of the tau neutrino mass. Our m_τ increases if the tau neutrino mass is greater than zero. By requiring consistency between this and the threshold measurements[3, 8] at the 1.64 standard deviation level, we derive a 95% confidence level upper limit on the tau neutrino mass of 71 MeV/c^2.

III. Electronic Branching Fraction

The method used for measuring $\mathcal{B}_e$ is based on counting e^+e^- annihilation events wherein *both* resulting taus decay to electrons, and normalizing to the number of tau pairs produced. This technique[15] directly measures $\mathcal{B}_e{}^2$, and hence errors in $\mathcal{B}_e$ are halved (except those involving individual track efficiencies). These events also provide an ideal territory to search for QED radiation that occurs during the decay process. There has been only one previous observation[16] of photons attributed to tau decay radiation, which was made in $\tau \to \mu\nu\bar{\nu}\gamma$ with low statistics. This work presents a conclusive observation of photons from electronic tau decay.

The branching fraction $\mathcal{B}_e$ is computed with

$$\mathcal{B}_e{}^2 = \frac{N_d\,(1 - f_{\tau\tau} - f_{ee} - f_{eeee} - f_{ee\tau\tau})}{\epsilon_t\,\epsilon_a\,\epsilon_e^2\,(1 + \delta)\,\sigma_o\,\Sigma_i(L_i/s_i)} \qquad (1)$$

where N_d is the number of events found in the data; the f's are background fractions from non-di-electron tau-pair decays ($f_{\tau\tau}$), $e^+e^-(\gamma\gamma)$ final states (f_{ee}), four electron final states (f_{eeee}), and two-photon tau-pair production ($f_{ee\tau\tau}$); ϵ_t is the trigger efficiency; ϵ_a is the acceptance for tau-pair di-electron decays; ϵ_e is the electron identification efficiency per particle; σ_o is the point cross section at s=1 GeV^2 (86.856 nb); $(1+\delta)$ is the factor correcting the point cross section for initial and final state radiation and the tau mass; and L_i is the measured integrated luminosity taken at center-of-mass energy $\sqrt{s_i}$ (in GeV). Each of these quantities is evaluated below, and is given with its statistical error appearing prior to its systematic error.

Radiative Bhabhas and two-photon events present potentially the largest background to di-electron tau-pair decays. Such events have other interacting particles in the final state which are either seen (as extra tracks or showers) or escape detection (by exiting near the beam line or overlapping with another particle). Conversely, electronic tau-pair decays have four unseen neutrinos which are not strongly collimated along either the initial or final state electron directions. These considerations lead to the following selection criteria. Two good charged tracks are required, each with $|\cos\theta| < 0.71$ and with scaled momentum $X_\pm = p_\pm c/E_{bm} > 0.1$. The acoplanarity ξ of the two tracks, defined as the azimuthal acollinearity in radians, must satisfy $0.15 < \xi < 1.5$. This forces some missing momentum away from the beam direction and each of the tracks, but does not allow two tracks to lie in the same hemisphere. The missing momentum must point at wide angles to the beam line ($|\cos\theta_{mis}| < 0.75$), and the component of the scaled missing momentum transverse to the beam must satisfy $X_t > 0.22$. No calorimeter shower of more than $0.1E_{bm}$ unassociated with a charged track is permitted. Finally, for electron identification, each track's calorimeter energy to drift chamber momentum ratio ("E/p") must

satisfy 0.85<E/pc <1.10, and its specific ionization in the drift chamber must be no more than two standard deviations below that expected for an electron. 3211 events satisfy all these requirements. By comparing the rates at which these events pass combinations of different online hardware triggers,[14, 17] the trigger efficiency ϵ_t=(98.99±0.13±0.23)% is determined.

The acceptance for Monte Carlo events is ϵ_a=(11.17±0.07±0.18)%. The dominant losses are from rejection on the basis of missing transverse momentum, polar angles of the tracks, and minimum track momentum. Two contributions are added in quadrature for the systematic error in ϵ_a: a relative ±1.0% uncertainty to account for possible inaccuracies in detector modeling, and a relative ±1.2% for simulation of tau decay. Decay radiation causes a relative efficiency reduction of ~10%, mostly due to the softening of the electron momentum spectrum.

The tau-pair total cross section multiplier, computed by KORALB to order α^3, is $(1+\delta)$=1.1783±0.0004±0.0118. The relative systematic error from α^4 corrections has been estimated[12] at ±1%. The Berends-Kleiss tau-pair generator[18] gives a consistent value for $(1+\delta)$.

The electron identification efficiency ϵ_e has been determined from a combination of radiative Bhabha events from the data, which provide several thousand tracks in every 250 MeV/c momentum bin, and Monte Carlo. The resulting efficiencies are ~99% for E/p < 1.10, ~99% for E/p > 0.85 and ~98% for the specific ionization requirement. Applying these efficiencies to the Monte Carlo tau-pair sample on a track-by-track basis on every event, the overall di-electron identification efficiency ϵ_e^2 can be computed, resulting in ϵ_e=(96.05±0.39)%. The error assigned to ϵ_e accounts for its small dependences on charge, momentum, polar angle, and time, as well as for the purity of the data sample selected to contain electrons.

The background predictions from four sources are modeled in Monte Carlo by the applicable event generator coupled with detector simulation.[13] Two-photon predictions[19] of f_{eeee}= (0.62 ±0.16 ±0.31)% and $f_{ee\tau\tau}$= (0.38 ±0.09 ±0.19)% account for topologies where two final state electrons escape at extreme polar angles. Annihilation into tau pairs[12] yields background when one tau decays to $e\nu\bar{\nu}$ but the other hadronically; in the result, $f_{\tau\tau}$= (0.63 ±0.15 ±0.32)%, the systematic error incorporates uncertainties in tau branching fractions and hadronic response[20] of the CLEO II detector and its simulation. Bhabha events were simulated with the BHLUMI[21] program, yielding f_{ee}=$(0.0^{+0.3}_{-0.0})$%.

There is a background cross-check available from the data. The angle

$$\Theta_M = \sin^{-1}[X_t/(\ 2\ -X_+\ -X_-\ )] \qquad (2)$$

is the minimum polar angle of unseen particles that preserves momentum and energy conservation. Tau-pair Monte Carlo and data are in excellent agreement for $\Theta_M > 10^\circ$ (a region populated by ~91% of the events), but there is an excess of 28±17 data events for $\Theta_M < 10^\circ$ (where there is no calorimeter coverage for vetoing extra particles). The $ee\gamma\gamma$, $eeee$, and $ee\tau\tau$ simulations predict $\sim 0^{+9}_{-0}$, ~17±5, and ~7±3 events, respectively, in this region, for a total of 24^{+11}_{-6} (statistical errors only), indicating Bhabha and two-photon backgrounds are adequately simulated. The systematic errors assigned to f_{eeee} and $f_{ee\tau\tau}$ account for possible discrepancies beneath the statistical power of this comparison.

The QED processes $e^+e^- \to e^+e^-$ and $e^+e^- \to \gamma\gamma$ are used to measure the luminosity. The analyses demand at least two showers with energy >0.5E_{bm} and $|\cos\theta| < 0.77$. Because electrons follow curved trajectories, the event is classified as an e^+e^- final state if the two showers have acoplanarity ξ >0.04; otherwise, and if there are no charged tracks, it is called $\gamma\gamma$. The visible cross sections of 11.77 nb and 1.222 nb at E_{bm}=5.29 GeV are computed with the applicable generators[21, 22] combined with detector simulation.[13] The Bhabha luminosity is ~1.5% smaller than the $\gamma\gamma$ result over all run periods. The weighted average of the e^+e^- and $\gamma\gamma$ measurements is 1.112 fb^{-1}. The systematic error on each of the two event rates is ±1.8%, which is dominated

for both processes by the luminosity variation with the $|\cos\theta|$ requirement. The polar angle distributions are shown in Fig. 2. The errors are correlated with each other because of their dependence on crystal response; the averaged Bhabha-$\gamma\gamma$ luminosity has precision $\pm 1.5\%$. Data were acquired at the $\Upsilon(4S)$ resonance ($\sqrt{s}$=10.58 GeV) and just below on the continuum ($\sqrt{s}$=10.52 GeV) in the ratio of $\sim$2:1 so that $\Sigma_i L_i/s_i = 9965 \pm 149$.

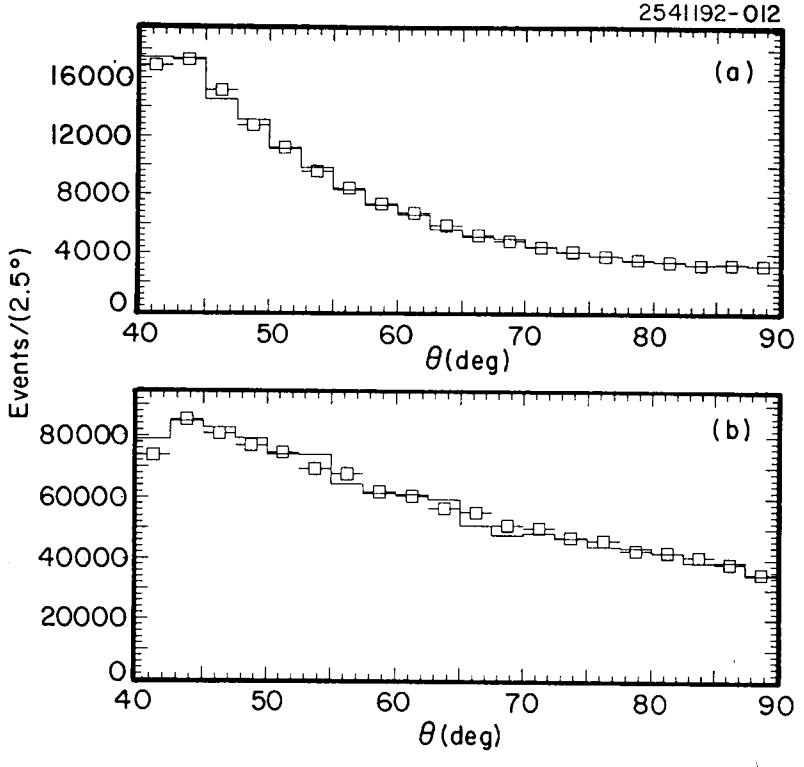

Fig. 2. Polar angle distributions for (*a*) Bhabhas, and (*b*) $\gamma\gamma$'s, used in the luminosity measurement for data (squares) and Monte Carlo (histograms).

The parameters used to compute $\mathcal{B}_e = 17.42 \pm 0.15 \pm 0.23$ are summarized in Table 2. The final errors in $\mathcal{B}_e$ are separated into the statistical error on the number of data events and the systematic error which includes all others, even those attributed to statistics in the lines above. The statistical error of slightly less than 1% and the systematic error of slightly more than 1% combine for a $\pm 1.6\%$ total error. The dominant contributions to the error, in descending order of importance, are Monte Carlo acceptance, luminosity, total cross section, and electron identification. Uncertainty in $\mathcal{B}_e$ from backgrounds and trigger efficiency are much smaller. This and the previous CLEO result[23] are independent measurements because they rely on data taken with different detectors.

Table 2: Parameters used to compute $\mathcal{B}_e$ and its errors

Name	Value	$\pm\sigma$(stat)	$\pm\sigma$(syst)	$\sigma(\mathcal{B}_e)/\mathcal{B}_e$(%)
N_d	3211	± 57		0.88
$f_{\tau\tau}$	0.0063	± 0.0015	± 0.0032	0.17
f_{eeee}	0.0062	± 0.0016	± 0.0031	0.17
$f_{eer\tau}$	0.0038	± 0.0009	± 0.0019	0.11
f_{ee}	0.000	± 0.003		0.15
ϵ_a	0.1117	± 0.0007	± 0.0018	0.84
ϵ_e	0.9605		± 0.0039	0.41
ϵ_t	0.9899	± 0.0013	± 0.0022	0.13
$(1+\delta)$	1.1783	± 0.0004	± 0.0121	0.51
$\Sigma L_i/s_i$	9965		± 149	0.75
$\mathcal{B}_e$	0.1742	± 0.0015	± 0.0023	1.60

The agreement between data and Monte Carlo for the kinematic variables involved in event selection is excellent as shown in Fig. 3. The value of $\mathcal{B}_e$ is quite stable with respect to alterations in selection criteria, detector calibration, and physics assumptions. When all selection criteria are loosened individually, or tightened alone or in concert, recomputing the efficiency and background for each case, the relative changes in $\mathcal{B}_e$ are less than $\pm 0.6\%$. The acceptance changes by $\Delta\epsilon_a/\epsilon_a = +11\%$ to -56% with these alternate event samples; the background subtraction doubles for some of the looser sets and halves for some

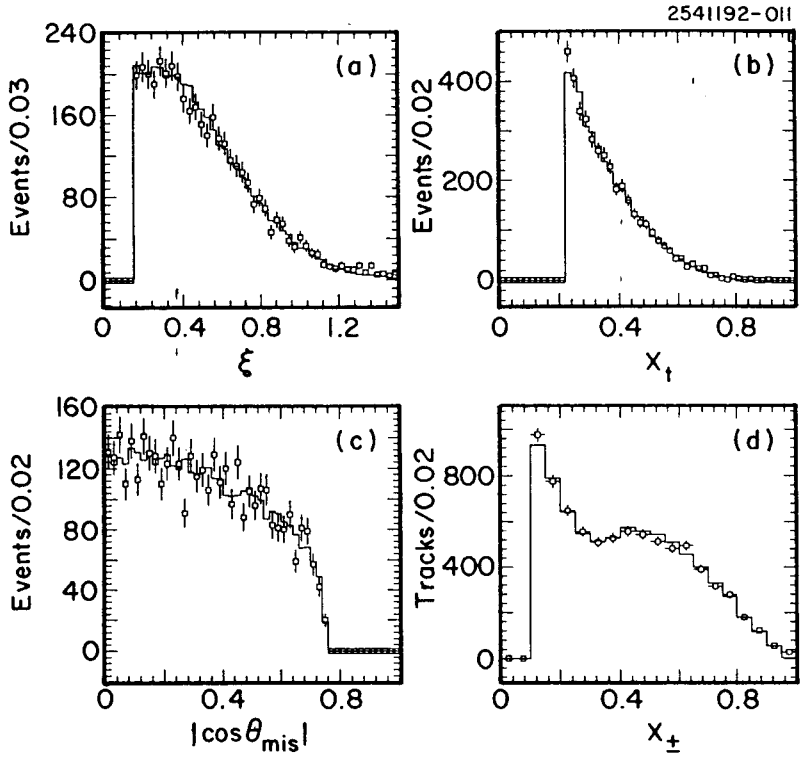

Fig. 3. Distributions in data (squares) and Monte Carlo (histograms) in (*a*) acoplanarity ξ, (*b*) scaled transverse momentum X_t, (*c*) $|\cos\theta_{\rm mis}|$, and (*d*) scaled electron momentum $X_\pm$ (two entries per event).

of the tighter ones. While the observed variations are consistent with statistical fluctuations in the data and uncertainties in the modified background subtractions, the systematic error in ϵ_a also accommodates such changes in $\mathcal{B}_e$. $\mathcal{B}_e$ has been computed separately for data taken in seven consecutive run periods of comparable luminosity. The seven values are statistically consistent with each other, as are the results confined to data taken below and on the $\Upsilon(4S)$ resonance. The effects of uncertainties in tau mass and tau neutrino mass are negligible. If the Michel parameter[3] were actually ρ=0.70 instead of the value predicted for a pure V−A current (0.75), the value for $\mathcal{B}_e$ presented here would need to be reduced by 0.9% of itself.

Using the recently measured tau mass[8] m_τ=(1776.9±0.4±0.3) MeV/c^2 and the value of $\mathcal{B}_e$ reported here, the Standard Model prediction[4] for the lifetime is τ_τ =(284.4±4.5) fs, substantially lower than recently quoted measurement averages of (305±6) fs[3] and (298.5±4.4) fs.[24] Should the discrepancy persist despite improved measurements, solving this puzzle would call for new physics.[4, 5]

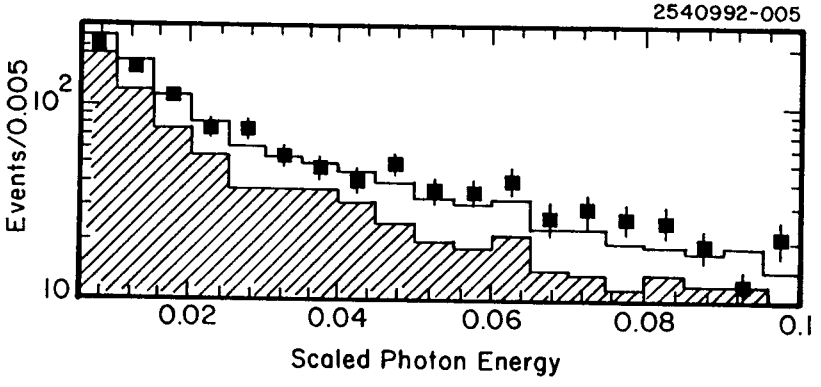

Fig. 4. Distribution of scaled photon energy for the highest energy isolated barrel shower per event in data (squares), Monte Carlo with decay radiation included (upper histogram) or excluded (hashed histogram). The bin with scaled photon energy <0.002, which has ~70% of the events, is suppressed.

The excellent agreement between the data and Monte Carlo in many variables gives some confidence that the decay radiative corrections are simulated correctly. The most convincing distribution is the energy spectrum of the highest energy photon per event with $|\cos\theta| < 0.8$ as shown in Fig. 4. Comparisons are quantified above scaled photon energy of 0.02 (~106 MeV) because

at such energies the number of fake photons expected is negligible; at lower energies random beam-related showers and satellites from the electron showers become significant. The Monte Carlo predicts 440±7±14 events with a photon exceeding this cutoff, and that the photons originate as decay radiation (186 events), bremsstrahlung in the detector material (180), initial/final state radiation (64), and from $\tau-$pair background (10). The number in the data, (453±21) events, is consistent with this prediction; it exceeds that predicted by Monte Carlo *without* decay radiation by 187±22±14 events, where the first error is statistical and the second includes uncertainty in the amount of material and background fractions. The absence of decay radiation is excluded by more than seven standard deviations.

In conclusion, a measurement of the tau lepton electronic branching fraction has been performed by normalizing di-electron events to luminosity. The value is consistent with and as precise as the previous world average.[3] The number and energy spectrum of photons in the di-electron sample agree with Monte Carlo only if tau decay radiation is included. This marks the first observation of $\tau \to e\nu\bar{\nu}\gamma$.

IV. Measurement of $\mathcal{B}(h^{\pm}\pi^0\nu)$

Here a precision measurement of $\mathcal{B}(h^{\pm}\pi^0\nu)$ is presented using the $h^+\pi^0\bar{\nu_\tau}$ vs. $h^-\pi^0\nu_\tau$ topology, where $h^{\pm}$ refers to either $\pi^{\pm}$ or $K^{\pm}$. The advantages of this double-tagging approach are that errors associated with event counting are halved and backgrounds from non-$\tau^+\tau^-$ events are readily made small. To fully exploit these advantages, it is important to understand the π^0 reconstruction efficiency as well as migration from other $\tau^+\tau^-$ topologies. The value for $\mathcal{B}(h^{\pm}\pi^0\nu)$ is calculated using a formula analogous to Eq. (1), except that the electron identification efficiency is not present, and the backgrounds are understood to be those applicable to this process.

The $h^{\pm}\pi^0\nu_\tau$ mode is dominated by $\rho^{\pm}\nu_\tau$, but also receives contributions from $K^*\nu_\tau$, $\rho'\nu_\tau$, and non-resonant $h^{\pm}\pi^0\nu_\tau$ modes. Modes containing an unobserved K_L or $\omega \to \gamma\pi^0$ are considered to be feed-across, *i.e.*, background for which a correction will be applied. The final branching ratio *does not include* such modes.

The dataset used for this measurement is the same as for m_τ above; the selection criteria only tighten those used in Section II except that $|S_{\gamma\gamma}| < 4$ (instead of 3), and showers unassociated with tracks or π^0's with $|\cos\theta| > 0.71$ must be less than 200 MeV (instead of 100). The tracks must have momentum exceeding $0.1E_{\rm bm}/c$. Each π^0 energy must exceed $0.1E_{\rm bm}$ after application of the mass constraint. Reconstructed π^0's are then associated with the charged particle nearest in space angle; each charged particle must have exactly one associated π^0. The visible energy of the $h^+\pi^0h^-\pi^0$ system must exceed $0.4E_{\rm cm}$ and the visible momentum transverse to the beam axis p_{t-vis} must exceed 200 MeV/c to suppress background from two-photon physics while accepting the signal events containing two unobserved neutrinos. Events are required to satisfy a subset of the possible CLEO triggers to ensure a reliable estimation of the trigger efficiency. A total of 6835 events pass these selection criteria. The trigger efficiency for these events is ϵ_t=0.988±0.001±0.006.

The $\pi^0 - \pi^0$ signal is then extracted from Fig. 5(a), where we plot the quantity $S_{\gamma\gamma}$ for one photon pair versus the other. The cut on $|S_{\gamma\gamma}|$ is loosened in this figure. We perform a two-dimensional fit to extract the $\pi^0\pi^0$ component from the remaining $\pi^0\gamma\gamma$ and $\gamma\gamma\gamma\gamma$ topologies. The fit function uses a Gaussian shape with a low-mass power-law tail to describe the non-Gaussian energy response of the calorimeter, and a linear background. Alternatively, signal and sideband regions are defined in which the signal region is defined by $|S_{\gamma\gamma}| < 4$ and a sideband subtraction performed. All these methods yield consistent results for the branching fraction, and the observed spread provides an estimate of the systematic error associated with the $\pi^0 - \pi^0$ signal extraction method. The sideband-subtraction method yields 6522 events, corresponding to a 4.5% non-$\pi^0\pi^0$ contribution within $|S_{\gamma\gamma}| < 4$.

The cuts described above were optimized to reduce systematic uncertainties, even at the expense of overall efficiency. Tight cuts are made on well-

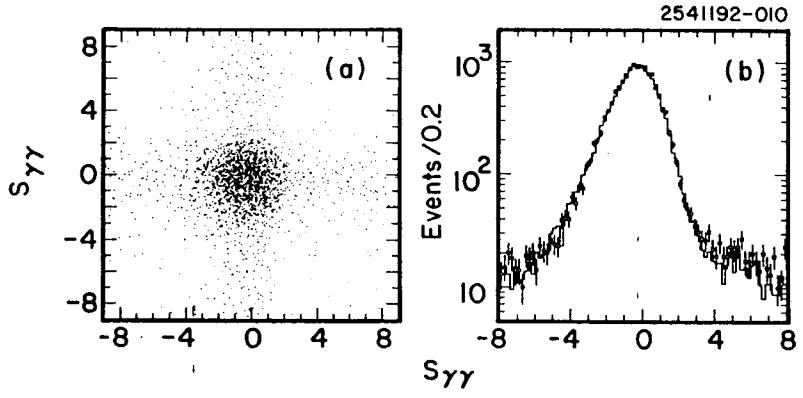

Fig. 5. (a) The quantity $S_{\gamma\gamma} \equiv (m_{\gamma\gamma} - m_{\pi^0})/\sigma_{\gamma\gamma}$ for one photon pair versus the other in the data. (b) The $S_{\gamma\gamma}$ distribution for the data (squares) and the Monte Carlo (histogram).

simulated kinematical quantities such as energies and angles of reconstructed particles. Looser cuts are applied on strongly detector-dependent quantities such as the presence of showers, which may result from hadronic interactions in the calorimeter. Because of this, feed-across from $\tau^+\tau^-$ modes with different π^0 topologies is not negligible, and must be estimated using the Monte Carlo simulation.

The overall reconstruction efficiency for the expected mix[3] of $\pi^\pm\pi^0$ and $K^\pm\pi^0$ modes is ϵ_a=0.0692±0.0008±0.0022, where the error is from Monte Carlo statistics and the second is systematic (examined below). This efficiency includes the $\mathcal{B}^2(\pi^0 \to \gamma\gamma)$. Also included are corrections for effects not well-simulated in the Monte Carlo. For example, the extra-photon veto efficiency depends on understanding hadronic shower in the CsI. An independent data sample of $\gamma\gamma \to 2(\pi^+\pi^-)$ events was studied to evaluate the accuracy of the simulation, resulting in an additional relative 1% correction.

The systematic error associated with this efficiency is evaluated by comparing distributions for a large range of kinematical variables between data and Monte Carlo. The π^0 signal and background shape, expressed in terms of the quantity $S_{\gamma\gamma}$, is shown in Fig. 5(*b*) for data and Monte Carlo. The GEANT-based detector simulation accurately simulates both the Gaussian core and non-Gaussian tails in the distribution. The distributions of several other kinematical variables are compared in Figs. 6(a)-(d). In these figures, we have applied a π^0 mass constraint to the neutral particles and energy loss corrections to the charged particles. Good agreement is seen in all cases.

All cuts on kinematical variables are varied over a wide range, including a variety of different extra shower veto criteria, and the resulting branching fraction is observed to be stable to within ±1.5% of itself. The data are split into nine subsamples in time, and also into subsamples collected on and off the $\Upsilon(4S)$ resonance. The variations in the resulting branching fractions are consistent within statistical fluctuations. From these studies, we estimate the relative systematic error on the reconstruction efficiency to be ±3%.

The following processes, with their estimated contributions to the final sample, were considered as sources of non-$\tau^+\tau^-$ background: $e^+e^- \to q\bar{q}$ where $q = u, d, s, c$ (0.25±0.08±0.08)%; $e^+e^- \to B\overline{B}$ (<0.04% at 90% confidence level); $e^+e^- \to e^+e^-\tau^+\tau^-$[25] (0.09±0.05±0.05)%; other two-photon (low-p_{t-vis}) processes (such as $e^+e^- \to e^+e^-\rho^+\rho^-$) (<0.95%, estimated by comparing the shapes of the E_{vis} and p_{t-vis} distributions between data and Monte Carlo).

To determine the amount of feed-across from other $\tau^+\tau^-$ modes, we use Monte Carlo for efficiencies for each mode. Ratios of branching fractions for multi-π^0 modes to that of the signal are estimated by averaging the values from reference 3 with the more precise results in Section V. The largest source of feed-across is from events of the topology $h^\pm\pi^0$ vs. $h^\mp\pi^0\pi^0$, which has efficiency 1.3%, about one-fifth of that for the signal. Taking into account the ratio of branching fractions, that mode constitutes 12% of the events from all $\tau^+\tau^-$ sources. The background fraction from all feed-across modes (including modes

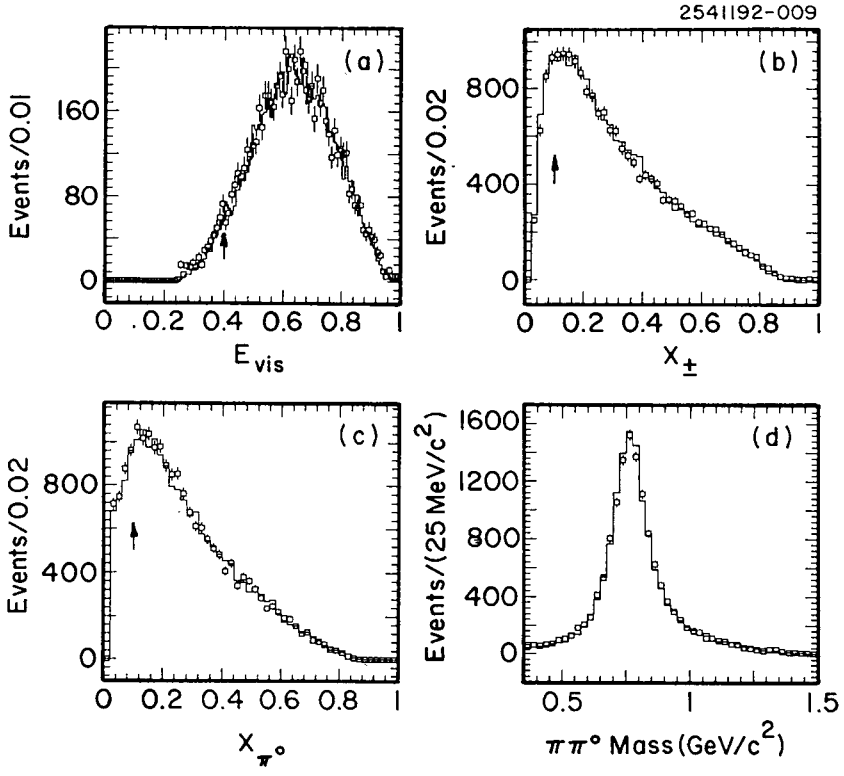

Fig. 6. Kinematical distributions for the data (squares) and for the KORALB Monte Carlo (histogram). Cuts are made on these quantities in $(a)-(c)$. The distribution is shown after all cuts except for the one in question, and the cut position is indicated. (a) the visible energy scaled to the beam energy; (b) the scaled momentum of the charged pions (**two entries per event**); (c) the scaled energy of the neutral pions (**two entries per event**); (d) the mass of the charged hadron (assumed to be a pion) and the π^0.

containing K_L, K_S, and $\omega \to \gamma\pi^0$ decays), is $(14.0 \pm 0.3 \pm 1.0)\%$, where the first error is from Monte Carlo statistics and the second from uncertainties in efficiencies for the feed-across modes and the assumed ratios of branching fractions.

The number of tau pairs produced is computed as in Section III. Because events with extra photons as low as 100 MeV are vetoed in this analysis, there is potentially extra sensitivity to the accuracy of the radiative corrections calculation. This leads to a more conservative theoretical error on $(1+\delta)$ of $\pm 1.5\%$.

With the parameters shown in Table 3, the branching ratio is calculated to be $\mathcal{B}(h^\pm\pi^0\nu) = 0.2483 \pm 0.0015 \pm 0.0053$ where the first error is statistical and the second systematic. This measurement is consistent with and more precise than the previous world average value.[3]

Table 3: Parameters used to compute $\mathcal{B}(h^\pm\pi^0\nu)$ and its error

Name	Value	$\pm\sigma$(stat)	$\pm\sigma$(syst)	σ(B)/B (%)
N_d	6522	± 81		0.62
$f_{\tau\tau}$	0.140	± 0.003	± 0.010	0.52
$f_{ee\tau\tau}$	0.0009	± 0.0005	± 0.0005	0.04
$f_{ee q\bar{q}}$	0.00		± 0.0095	0.48
$f_{q\bar{q}}$	0.0025	± 0.0008	± 0.0008	0.06
ϵ_a	0.0692	± 0.0008	± 0.0022	1.69
ϵ_t	0.989	± 0.001	± 0.006	0.30
$(1+\delta)$	1.1783	± 0.0004	± 0.0177	0.75
$\Sigma L_i / s_i$	12812		± 192	0.75
$\mathcal{B}(h^\pm\pi^0\nu)$	0.2483	± 0.0015	± 0.0053	2.22

The measured branching fraction includes contributions from the decay $\tau^\pm \to K^{*\pm}\nu_\tau$, where $K^{*\pm} \to K^\pm\pi^0$. Using the world average for the former decay branching fraction,[3] and assuming no other contributions to the signal, we determine $\mathcal{B}(\pi^\pm\pi^0\nu_\tau) = 0.2435 \pm 0.0055$. Normalizing to the new CLEO II electronic branching fraction (presented in Section III), $\mathcal{B}(\pi^\pm\pi^0\nu_\tau)/\mathcal{B}_e = 1.40 \pm 0.03$. This agrees with the CVC prediction[11, 4] of $\mathcal{B}(\pi^\pm\pi^0\nu_\tau)/\mathcal{B}_e = 1.33 \pm 0.07$ (updated for the recent tau mass measurements[7, 8]).

V. Measurement of $\mathcal{B}(h^{\pm}n\pi^0\nu)$

To study multi-π^0 single-prong τ decays, we identify the decay of the recoiling ('tag') τ. There are two independent analyses, one using leptonic ($e\nu\overline{\nu}$, $\mu\nu\overline{\nu}$) tags; and one using three-prong ($3h^{\pm}[\pi^0]\nu$) tags. Events with 1-1 and 1-3 charged track topologies and zero net charge are selected. The opening angle between the charged tracks in the 1-1 topology must exceed 90°; 1-3 events are divided into two hemispheres by the plane perpendicular to the axis defined by the highest momentum track. Only one track may have more than $0.85E_{bm}$, and at least two tracks must project back to the e^+e^- interaction point. For leptonic (3-prong) tags, the total energy deposited in the calorimeter must be less than $0.85E_{cm}$ ($0.75E_{cm}$), and the total visible energy E_{vis} must exceed $0.2E_{cm}$ ($0.3E_{cm}$), assuming observed charged particles to be pions. The data sample used corresponds to integrated luminosity of 670 pb^{-1}, corresponding to ~ 0.61M produced $\tau^+\tau^-$ pairs.

Electrons are identified above 0.5 GeV/c as in Section III. Muons above 1.0 GeV/c are found by projecting tracks to hits in muon counters located behind at least three absorption lengths of iron. QED backgrounds to the lepton tag sample are minimized by requiring the net missing momentum to point into the detector, the net transverse momentum of the tracks to exceed 200 MeV/c, and the ratio of the vector- to scalar-sum of the charged track momenta to exceed 0.05. For three-prong-tagged events, hadronic background is suppressed by requiring that the event missing mass, $[\,(E_{cm}- E_{vis})^2 - \vec{p}^{\,2}_{vis}]^{1/2}$, be between 0.5 and 7.0 GeV/c^2. Radiative Bhabha events with converted photons are rejected by allowing no more than one identified electron.

Candidate photons are formed from clusters of crystal hits for the barrel ($|\cos\theta| < 0.80$) and endcap ($0.8 < |\cos\theta| < 0.95$) regions of the calorimeter. Clusters associated with charged particles are ignored, and we reject events with appreciable energy deposition in the endcaps. The criteria for photons and π^0 reconstruction depend on the type of tag. For three-prong-tagged events, barrel (endcap) clusters of energy $E_\gamma > 60\,(100)$ MeV are partitioned according to the hemispheres defined by the tracks. The three-prong hemisphere may contain no more than two such photons, and the invariant mass of all detected particles in each hemisphere must be less than 1.7 GeV/c^2. The net momentum in each hemisphere must also point into the barrel region. We form π^0's using only barrel photons in the one-prong hemisphere and reject events having unused barrel photons of energy above 60 MeV.

In the lepton-tagged analysis, photons used to reconstruct π^0's must lie in the barrel and have $E_\gamma > 60$ MeV, except for the $\tau \to h^{\pm}4\pi^0\nu_\tau$ decay, where photons as soft as 30 MeV are used. Photons within 20° of electron or muon initial directions are ignored. Photons forming π^0's must satisfy the following requirements: at least one photon must have $E_\gamma > 80$ MeV; the angle between the two photons must be $< 135°$; the momentum vector of each π^0 candidate must lie within 90° of the charged pion direction; and the energy of any unused barrel photon may not exceed 100 MeV. A candidate event picture for a μ^- vs. $\pi^+3\pi^0$ event is shown in Fig. 7.

For each π^0 multiplicity hypothesis, the combination of π^0 candidates in an event with the lowest value of the "reduced $n\pi^0$ χ^{2}" is chosen, where $\chi^2_{n\pi^0} = \frac{1}{n}\sum_{i=1}^{n}(m_i - m_{\pi^0})^2/\sigma^2_{m_i}$. Here m_i is the effective mass of the two photons forming the i^{th} π^0 candidate, and σ_{m_i} is the uncertainty on m_i (typically 6-8 MeV/c^2). Finally, an event must satisfy a loose $(\chi^2_{n\pi^0})_{min}$ cut to survive as a candidate. The $\pi^{\pm}(n\pi^0)$ invariant mass spectra for events from all tags are shown in Fig. 8.

Table 4 gives, for each tag and each π^0 multiplicity, the number of events found in the data, background fractions, efficiency relative to $\mathcal{B}(h^{\pm}\pi^0\nu)$, and $\mathcal{B}(h^{\pm}n\pi^0\nu)/\mathcal{B}(h^{\pm}\pi^0\nu)$. The contamination from events in which unrelated photons form a π^0 candidate (f_{π^0}) is evaluated from the tails of the χ^2 distributions. After subtraction of this background, hadronic background (f_h) for the lepton-tagged sample is estimated from a Monte Carlo simulation. In order to determine f_h for the three-prong-tagged sample, from the data we select hadronic events with criteria identical to the 1-3 tau-pair selection described

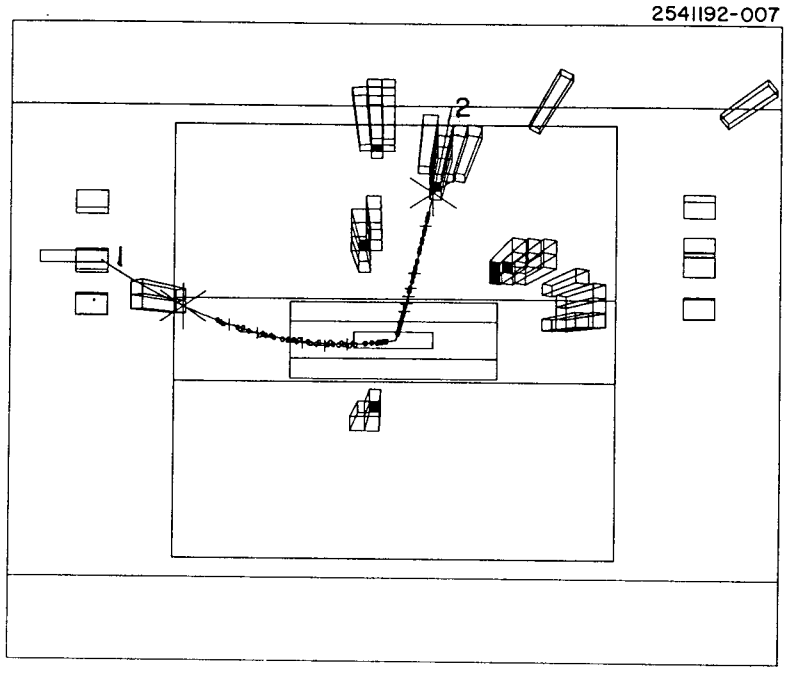

Fig. 7. Side view of μ^- vs. $\pi^+3\pi^0$ event in the CLEO II detector. The μ^- is shown coming out of the page toward the left and is labelled as track 1.

earlier, except that the mass of the $3h^{\pm}$ candidate must exceed 2.0 GeV/c^2, and any number of photons is permitted in the three-prong hemisphere. Since the correlation between the mass distributions of the two hemispheres is small, we obtain the hadronic background in the three-prong-tagged sample by normalizing the one-prong mass (M_1) spectrum of the hadronic events to the one-prong mass spectrum of the τ candidates in the region $M_1 > 2.0$ GeV/c^2, which is dominated by hadrons.

Branching fractions for the multi-π^0 τ decays are computed using the numbers of selected events and efficiencies, and background contributions listed in

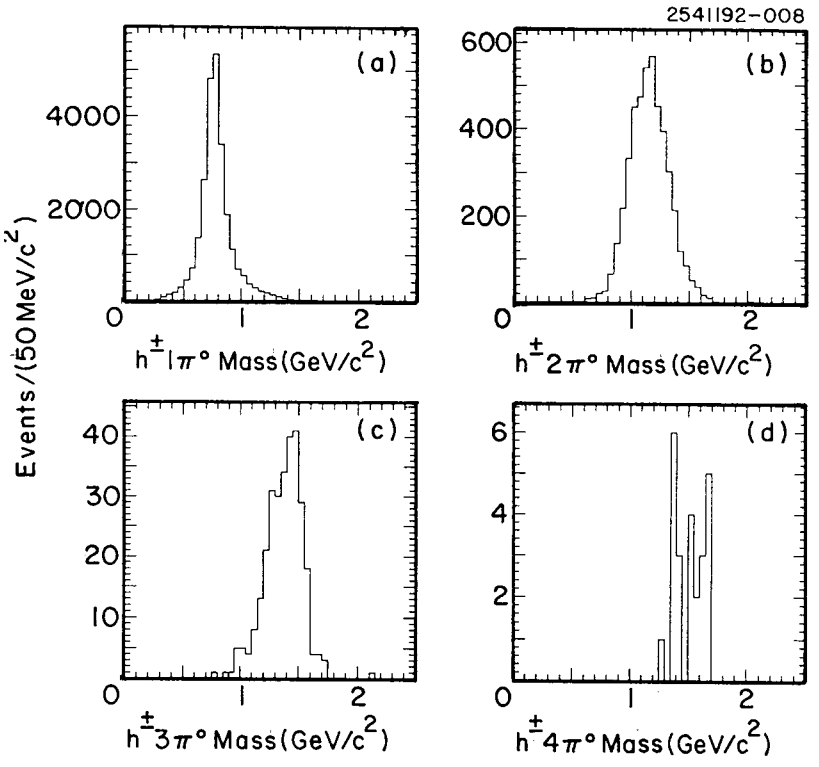

Fig. 8. Invariant $h^{\pm}n\pi^0$ mass spectra. Data from leptonic and three-prong tags are combined for events in the 1-, 2-, and 3-π^0 samples. Only lepton-tagged events are shown for the $4\pi^0$ case.

Table 4. Since the ratios of the multi-π^0 branching fractions enter explicitly in the estimate of f_τ', we iterate until consistency is reached.[26] The final column of Table 4 lists the resulting ratios of branching fractions.

The dominant source of systematic uncertainty for both leptonic and three-prong-tagged analyses is the $n\pi^0$-finding efficiency. The uncertainty in this efficiency arises from possible deficiencies in the Monte Carlo simulation of photon and hadronic interactions in the calorimeter. The overall uncertainty is

Table 4: Parameters with statistical errors for the $\mathcal{B}(h^{\pm}n\pi^0\nu)$

Mode (X)	Tag	Evts.	f_{π^0}	f_h	f_τ	Relative Eff.(%)	$\frac{\mathcal{B}(h^{\pm}n\pi^0\nu)}{\mathcal{B}(h^{\pm}\pi^0\nu)}$
$h^{\pm}\pi^0\nu$	e	8935	2.2 ± 0.1	< 0.1	3.8 ± 0.1	100	1
	μ	7470	2.3 ± 0.1	< 0.1	3.9 ± 0.1	100	1
	$3h$	8603	1.9 ± 0.2	2.7 ± 0.1	2.7 ± 0.3	100	1
$h^{\pm}2\pi^0\nu$	e	1639	4.1 ± 0.3	< 0.4	2.6 ± 0.2	53.9 ± 0.7	0.337 ± 0.009
	μ	1434	3.7 ± 0.3	< 1.0	2.6 ± 0.2	53.5 ± 0.8	0.360 ± 0.011
	$3h$	1439	4.8 ± 0.7	3.9 ± 0.3	0.5 ± 0.5	46.4 ± 1.7	0.352 ± 0.012
$h^{\pm}3\pi^0\nu$	e	111	11 ± 2	< 6	8.6 ± 1.3	25.5 ± 2.0	0.042 ± 0.005
	μ	100	11 ± 2	< 6	8.4 ± 1.6	26.4 ± 0.7	0.044 ± 0.005
	$3h$	85	14 ± 6	16 ± 3	2.5 ± 1.0	18.8 ± 1.7	0.039 ± 0.006
$h^{\pm}4\pi^0\nu$	e	9	14 ± 6	< 10	4.3 ± 2.3	18.8 ± 1.2	0.005 ± 0.002
	μ	12	15 ± 6	< 10	4.3 ± 2.3	16.7 ± 1.4	0.008 ± 0.003
	$3h$	4	50 ± 25	25 ± 25	3 ± 3	8.3 ± 1.7	< 0.01

determined by varying the energy, angle and multiplicity requirements imposed on photons. The π^0-finding efficiency is checked by performing a semi-inclusive analysis of $B_{h2\pi^0}/B_{h\pi^0}$ ($B_{h3\pi^0}/B_{h\pi^0}$) in which the Monte Carlo and data energy spectra of unused photons are compared for events in which one (two) π^0's have been reconstructed. From these studies we estimate π^0 reconstruction uncertainties of 4.1%, 8.1%, and 30% for the 2-, 3-, and 4-π^0 results, respectively.

The error due to the π^0 signal extraction method is estimated by comparing the results of n-dimensional sideband subtractions to the χ^2 method, and also by considering all π^0 combinations instead of only the "best" one. Uncertainties in modeling the trigger efficiency are determined from the data, comparing parallel trigger streams with different energy and tracking requirements. Systematic errors in the hadronic background subtraction are obtained from studies of (hadron-dominated) 3-3 topology events selected with the same criteria as the 1-3 events. The τ background subtraction is studied by varying the input branching ratios used in the τ Monte Carlo over a range permitted by existing measurements.[3] For $B_{h3\pi^0}/B_{h\pi^0}$, significant contributions to the overall systematic error arise from signal extraction (5.5%) and τ background (5.0%).

The results from the different tags are averaged, weighted by statistical and independent systematic errors added in quadrature. Errors due to signal extraction, π^0 reconstruction, and f_τ are added in quadrature with the independent systematic errors. The resulting branching fraction ratios are $\mathcal{B}(h^{\pm}2\pi^0\nu)/\mathcal{B}(h^{\pm}\pi^0\nu)$= 0.348 $\pm$0.006 $\pm$0.016, $\mathcal{B}(h^{\pm}3\pi^0\nu)/\mathcal{B}(h^{\pm}\pi^0\nu)$= 0.042 $\pm$0.003 $\pm$0.004, and $\mathcal{B}(h^{\pm}4\pi^0\nu)/\mathcal{B}(h^{\pm}\pi^0\nu)$= 0.006 $\pm$0.002 $\pm$0.002, where the first error is statistical and the second systematic.

Using the new world average value $\mathcal{B}(h^{\pm}\pi^0\nu)$= 0.2426 $\pm$0.0041, which combines Ref. 3 with the more recent ARGUS[27] and CLEO (Section IV) values, the absolute branching fractions become $\mathcal{B}(h^{\pm}2\pi^0\nu)$= 0.0844 $\pm$0.0015 $\pm$0.0039 $\pm$0.0014, $\mathcal{B}(h^{\pm}3\pi^0\nu)$= 0.0102 $\pm$0.0007 $\pm$0.0010 $\pm$0.0002, and $\mathcal{B}(h^{\pm}4\pi^0\nu)$= 0.0015 $\pm$0.0005 $\pm$0.0005 $\pm$0.0001, where the last uncertainty reflects that of $\mathcal{B}(h^{\pm}\pi^0\nu)$. These results are consistent with and more precise than the current world averages. They are all smaller than previous world averages in Ref. 3, however, supporting the existence of the one-prong problem. In particular, the branching fraction for $\tau \to h^{\pm}2\pi^0\nu_\tau$ is markedly lower than some recent experiments.[28, 29] The branching fractions for the $h^{\pm}3\pi^0\nu$ and $h^{\pm}4\pi^0\nu$ modes are consistent with theoretical expectations from CVC and isospin.[2, 30]

VI. Conclusions

New, preliminary measurements from CLEO II of the tau mass, electronic branching fraction, and branching fractions to a single charged hadron accompanied by one, two, three, or four explicitly reconstructed π^0's have been presented. All the branching fractions are determined with unprecedented precision. The consistency problem is reduced by the smaller tau mass, but the lower value of $\mathcal{B}_e$ and its smaller errors maintain the discrepancy at more than two standard deviations. More precise (and smaller) values of $\mathcal{B}(h^{\pm}n\pi^0\nu)$, n=1-4, do not help the one-prong problem either, though the magnitude of the deficit depends in detail on how different experimental results are combined. Further measurements of these quantities, as well as the lifetime and other

branching fractions, are needed to understand these discrepancies.

VII. Acknowledgements

We gratefully acknowledge the effort of the CESR staff in providing us with excellent luminosity and running conditions. Credit for the individual analyses goes to Alan Weinstein for the tau mass and $\mathcal{B}(h^{\pm}\pi^0\nu)$ measurements, and to Glen Crawford, K.K. Gan, and Jon Urheim for the $\mathcal{B}(h^{\pm}n\pi^0\nu)$ determinations. This work was supported by the National Science Foundation and the U.S. Dept. of Energy.

REFERENCES

1. T. N. Truong, Phys. Rev. D **30**, 1509 (1984).
2. F.J. Gilman and S.H. Rhie, Phys. Rev. D **31**, 1066 (1985).
3. Particle Data Group, K. Hikasa *et al.*, "Review of Particle Properties." Phys. Rev. D **45** Part II, 1 (1992).
4. W.J. Marciano, Phys. Rev. D **45**, 721 (1992).
5. E. Ma, S. Pakvasa, and S.F. Tuan, PARTICLE WORLD Vol. 3, No. 1, 27 (1992).
6. Further analysis has resulted in: $\mathcal{B}_e$=0.1749±0.0014±0.0022 as explained in CLEO Collab., D.S. Akerib *et al.*, Cornell Univ. Laboratory of Nuclear Studies preprint CLNS 92/1163, Sept. 1992 (submitted to Phys. Rev. Lett.); and $\mathcal{B}(h^{\pm}2\pi^0\nu)/\mathcal{B}(h^{\pm}\pi^0\nu)$=0.345±0.006±0.016, $\mathcal{B}(h^{\pm}3\pi^0\nu)/\mathcal{B}(h^{\pm}\pi^0\nu)$=0.041±0.003±0.005, and $\mathcal{B}(h^{\pm}4\pi^0\nu)/\mathcal{B}(h^{\pm}\pi^0\nu)$= 0.006±0.002±0.002, as presented in CLEO Collab., M. Procario *et al.*, Cornell Univ. Laboratory of Nuclear Studies preprint CLNS 92/1165, Sept. 1992 (submitted to Phys. Rev. Lett.).
7. ARGUS Collab., H. Albrecht *et al.*, DESY preprint DESY-92-086 (June 1992); see also the presentation of B. Spaan in these proceedings.
8. BES Collab., J.Z. Bai *et al.*, Stanford Linear Accelerator Center preprint SLAC-PUB-5870 (June 1992) (submitted to Phys. Rev. Lett.); see also the presentation of E. Soderstrom in these proceedings.
9. Y.S. Tsai, Phys. Rev. D **4**, 2821 (1971); T. Kinoshita and A. Sirlin, Phys. Rev. **113**, 1652 (1958).
10. W. Marciano and A. Sirlin, Phys. Rev. Lett. **61**, 1815 (1988).
11. J. Kühn and A. Santamaria, Z. Phys. C **48**, 443 (1990).
12. KORALB v. 2.1/TAUOLA v. 1.5: S. Jadach and Z. Was, Comp. Phys. Comm. **36**, 191 (1985); S. Jadach and Z. Was, Comp. Phys. Comm. **64**, 267 (1991); S. Jadach, J.H. Kuhn, and Z. Was, Comp. Phys. Comm. **64**, 275 (1991); M. Jezabek, Z. Was, S. Jadach, and J.H. Kuhn, CERN-TH-6195-91 (Aug. 1991).
13. R. Brun *et al.*, GEANT v. 3.14, CERN DD/EE/84-1.
14. CLEO Collab., Y. Kubota *et al.*, Nucl. Instrum. Methods A **320**, 66 (1992).
15. Mark III Collab., R.M. Baltrusaitis *et al.*, Phys. Rev. Lett. **55**, 1842 (1985).
16. Mark II Collab., D.Y. Wu *et al.*, Phys. Rev. D **41**, 2339 (1990).
17. C. Bebek *et al.*, Nucl. Instrum. Methods A **302**, 261 (1991).
18. F. Berends and R. Kleiss, Nucl. Phys. **B177**, 237 (1981).
19. J. Vermasseren, Nucl. Phys. **B229**, 347 (1983).
20. Tau pairs from the data in the 1-vs-1 prong topology were used to measure a rejection of ~4:1 for the specific ionization requirement on tracks selected *not* to be electrons with E/p<0.5. An E/p rejection of ~75:1 was measured with pions from reconstructed $\rho^{\pm}$'s in the 1-vs-1 topology, as well as with pions from hadronic events isolated with tight specific ionization criteria.

21. S. Jadach, E. Richter-Was, B.F.L. Ward, and Z. Was, CERN-TH-6230-91 (Sept. 1991); S. Jadach, E. Richter-Was, B.F.L. Ward, and Z. Was, Phys. Lett. B **268**, 253 (1991); S. Jadach and B.F.L. Ward, Phys. Rev. D **40**, 3582 (1989); S. Jadach, E. Richter-Was, B.F.L. Ward, and Z. Was, Phys. Lett. B **260**, 438 (1991); S. Jadach, E. Richter-Was, B.F.L. Ward, and Z. Was, Phys. Lett. B **253**, 469 (1991). The *s*-channel diagrams have been added to the program.

22. F. Berends and R. Kleiss, Nucl. Phys. **B186**, 22 (1981); F. Berends and R. Kleiss, Nucl. Phys. **B228**, 537 (1983).

23. CLEO Collab., R. Ammar *et al.*, Phys. Rev. D **45**, 3976 (1992).

24. J. Harton, "Results on the Tau at LEP, "reported at the SLAC Summer Institute, Stanford, California (July 13-24, 1992), and in these proceedings.

25. V.M. Budnev *et al.*, Phys. Rep. **C15**, (1975) 181.

26. We also take $B(\tau \to h^{\pm}K^0\pi^0\nu_\tau) = (0.48 \pm 0.48)\%$, based on related decays summarized in Ref. 3. For the $h^{\pm}4\pi^0\nu$ final state we only consider "feedup" from modes with lower π^0 multiplicity, so the result may include contributions from final states such as $h^{\pm}5\pi^0\nu$.

27. ARGUS Collab., H. Albrecht *et al.*, DESY preprint DESY-92-082, June 1992.

28. ALEPH Collab., D. Decamp *et al.*, Z. Phys. C **54**, 211 (1992).

29. CELLO Collab., H.J. Behrend *et al.*, Z. Phys. C **46**, 537 (1990).

30. The $h^{\pm}4\pi^0\nu$ result includes a contribution from the decay $\tau^{\pm} \to \pi^{\pm}\eta\pi^0\nu_\tau$, with $\eta \to \pi^0\pi^0\pi^0$. This contribution is expected to be $(0.06 \pm 0.01)\%$, based on the direct study of this τ decay channel using $\eta \to \gamma\gamma$, $\pi^+\pi^-\pi^0$, and $\pi^0\pi^0\pi^0$; see CLEO Collab., M. Artuso *et al.*, Cornell Preprint CLNS 92/1159, (1992).